Compositionally Asymmetric Tri-Color Superlattices Grown by Pulsed Laser Deposition

H. N. Lee, H. M. Christen, C. M. Rouleau, S. Senz[1], S. K. Lee[1], D. Hesse[1], and D. H. Lowndes
Condensed Matter Sciences Division, Oak Ridge National Laboratory,
Oak Ridge, TN 37831, USA
[1]Max-Planck-Institut für Mikrostrukturphysik, Weinberg 2, D-06120 Halle/Saale, Germany

ABSTRACT

Compositionally asymmetric tri-color superlattices (TCS) with a combination of $BaTiO_3/SrTiO_3/CaTiO_3$ have been grown by pulsed laser deposition (PLD) on atomically-flat $SrRuO_3$-covered (001) $SrTiO_3$ substrates. Conducting $SrRuO_3$ films with single-terrace steps that closely mimic those of the $SrTiO_3$ substrate also were grown by PLD and serve as bottom electrodes. In order to achieve atomic control of each layer, we have calibrated precisely the number of laser pulses required to grow one unit-cell-thick layers (~200 for a laser spot of 0.4 mm^2). These conditions allowed recording of pronounced oscillations of the reflection high-energy electron diffraction (RHEED) specular spot intensity over the entire growth run - even for TCS layers totaling more than 1000 nm in total thickness.

INTRODUCTION

Advances in modern epitaxial growth techniques have enabled the growth of nearly perfect thin films, superlattices, etc. by the atomic-scale control of surfaces and interfaces. For instance, oxide heterostructures with atomically-flat interfaces and single unit-cell steps on the surface can be grown on well-prepared single-stepped substrates. Moreover, artificial superlattices – i.e., materials that do not exist in bulk forms – can be grown with great control on such substrates and are expected to result in unprecedented physical properties. Epitaxial thin films with arbitrary (but precisely controlled) stacking of layers with an A/B/C/…A/B/C geometry - so called tri-color or three-component superlattices (TCS), cf. Fig. 1 - can exhibit compositionally-broken inversion symmetry (CBIS), which results in strong self-poling due to the ionic size and/or electrostatic interaction effects by the isovalent and heterovalent substitutions, respectively [1]. Consequently, TCSs with CBIS may result in anomalous piezoelectricity and dielectric responses, and will allow a wide tunability of ferroelectric properties [2]. The growth of atomically-flat layers, however, is not trivial due

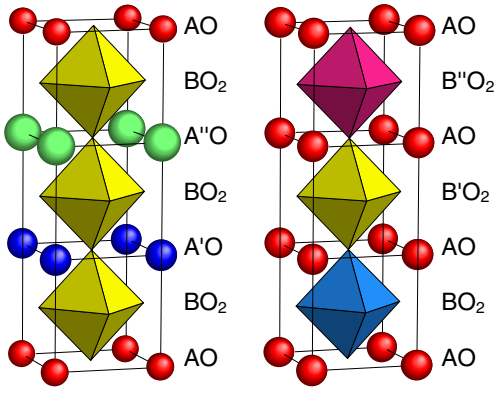

Figure 1. Tri-color superlattices of *A*-site $[(A_{1/3}A'_{1/3}A''_{1/3})BO_3]$ (left) and *B*-site $[A(B_{1/3}B'_{1/3}B''_{1/3})O_3]$ (right) substitutions. The inversion symmetry is broken by either isovalent or heterovalent substitution.

to lattice misfit, different growth modes, and lack of atomically-flat conducting layers for electric characterization. For example, growing $BaTiO_3$ on $SrTiO_3$ (misfit ~2%) involves the layer-then-island growth mechanism which usually destroys the sharpness of subsequent interfaces if the $BaTiO_3$ thickness exceeds two unit cells [3]. Thus, in order to design and fabricate functional materials and structures thereof, it is paramount that systematic studies be carried out on the growth behavior of transition metal oxides.

Here we report the growth control of TCSs consisting of $BaTiO_3$, $SrTiO_3$, and $CaTiO_3$ with atomically flat interfaces and surfaces on $SrRuO_3$-coated $SrTiO_3$ substrates.

EXPERIMENTS

Before growing TCSs, $SrRuO_3$ films were grown by PLD on single-stepped (001) $SrTiO_3$ substrates (cf. Fig. 2a) using a KrF excimer laser (λ = 248 nm) at 700 °C in 100 mTorr O_2. The single-stepped $SrTiO_3$ substrates were prepared by dipping as-purchased $SrTiO_3$ (miscut tolerance < 0.1°) in NH_4F-buffered-HF (BHF) (pH=4.5, BHF: H_2O = 1:10) for 30–60 sec followed by thermal anneal at 1100–1200 °C depending on the miscut angle of the substrates. After characterizing the surface of $SrRuO_3$ films by atomic force microscopy (AFM) in air, the samples were bonded onto a sample holder with Ag paint and reloaded in a different vacuum chamber equipped with reflection high-energy electron diffraction (RHEED) for in-situ surface monitoring. The TCSs were grown by PLD at ~700 ^{o}C in 10 mTorr of oxygen. The laser repetition rate was varied from 1 to 20 Hz for the optimization phase and fixed finally at 5 Hz. The laser fluence was fixed at 2 J/cm^2. The RHEED system was used at relatively high background pressure (up to tens mTorr) by differential pumping the e-gun filament with a large capacity turbo pump (pumping speed ≈ 300 *l*/s), which kept the pressure in the e-gun to less than 5×10^{-6} Torr. Sintered stoichiometric $CaTiO_3$ and $BaTiO_3$ targets, and a single-crystal $SrTiO_3$ target were used for growing the TCSs. The orientation, crystallinity, and strain state of TCSs were characterized by x-ray diffraction (XRD) θ–2θ and two-axes (reciprocal space map) scans using a PANalytical X'Pert MRD four-circle diffractometer.

RESULTS AND DISCUSSION

Atomically-flat, single-stepped $SrTiO_3$ substrates were prepared as described above. Figure 2(a) shows a treated $SrTiO_3$ substrate used for growing $SrRuO_3$ thin films. The corresponding AFM topographic image of the $SrRuO_3$ film [Fig. 2(b)] grown on the $SrTiO_3$ substrate also displays a nearly atomically-flat surface with uniform single steps. The terrace widths are more or less identical to the $SrTiO_3$ substrate. We have not recorded RHEED oscillations during $SrRuO_3$ growth due to the high pressure involved. Furthermore, RHEED would yield limited information beyond a few monolayers of film deposition because the growth mode at relatively high oxygen pressure quickly changes from layer-by-layer to step-flow [4].

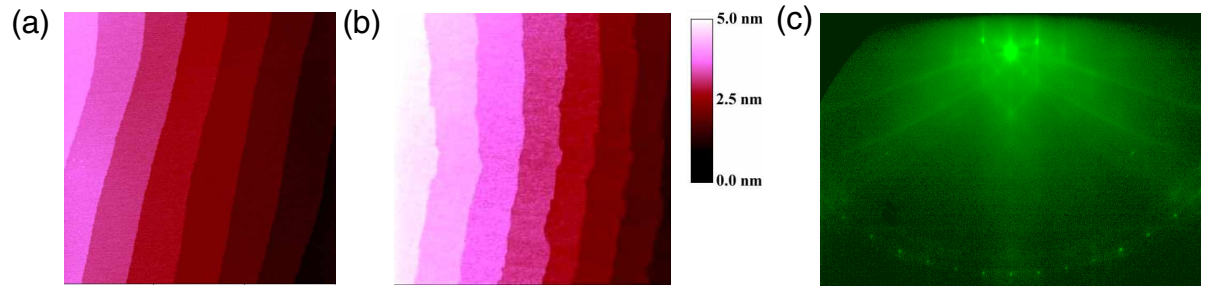

Figure 2. AFM topography images (image size: 3×3 μm^2) of (a) a (001) $SrTiO_3$ substrate and (b) a $SrRuO_3$ film grown on the (001) $SrTiO_3$ substrate with uniform single terrace steps. (c) RHEED screen image of a $SrRuO_3$ film with the well-defined bright specular spot and the secondary Laue pattern along the <100> direction.

The nearly atomically-flat surface of the $SrRuO_3$ film also is confirmed by the ex-situ RHEED image shown in Fig. 2(c). The RHEED image was taken along the <100> direction of $SrRuO_3$ and showed a very bright specular spot and diffraction spots, as well as the secondary Laue pattern, all revealing a high quality $SrRuO_3$ surface.

Since $CaTiO_3$ and $SrTiO_3$ both exhibit the layer-by-layer growth mode, and $BaTiO_3$, the layer-then-island growth mode, pronounced RHEED intensity oscillations were observed over the entire growth of $CaTiO_3$ and $SrTiO_3$, and at least few from $BaTiO_3$. This made it possible to calibrate accurately the number of laser pulses required to grow unit cells of $CaTiO_3$, $SrTiO_3$, and $BaTiO_3$ by counting the number of laser pulses necessary for one RHEED specular spot oscillation. Figure 3 shows how we have calibrated precisely the number of laser pulses. As shown in Fig. 3(a), apertures of different sizes were placed on a imaging beamline to achieve different laser spots (#1 = 7.7 mm^2, #2 = 2.0 mm^2, #3 = 1.1 mm^2, and #4 = 0.4 mm^2). Even with a small spot, the top edge of the laser plume reached the substrate surface. More importantly, small spots enable precise control of number of unit cells and highly consistent RHEED specular spot oscillations as shown in Fig. 3(b). In 0.4 mTorr O_2 background pressure, for instance, 19 laser pulses are required for growing one unit cell of $SrTiO_3$ when aperture #2 is used, whereas 148 laser pulses are required with aperture #4. At 10 mTorr, however, more laser pulses are needed due to increased collision and scattering of the ablated species [e.g., 190 laser pulses are needed for ~0.4 nm thick $SrTiO_3$ (1 u.c.)]. It turned out that growing with a larger aperture requires a reduction in laser repetition rate in order to allow enough migration time of species arriving on the substrate surface to nucleate before the successive species arrive. Under these conditions, the RHEED oscillation was pronounced, but layer coverage was difficult to control. Consequently, the smallest aperture (#4) was employed in order to control the layer thickness more precisely.

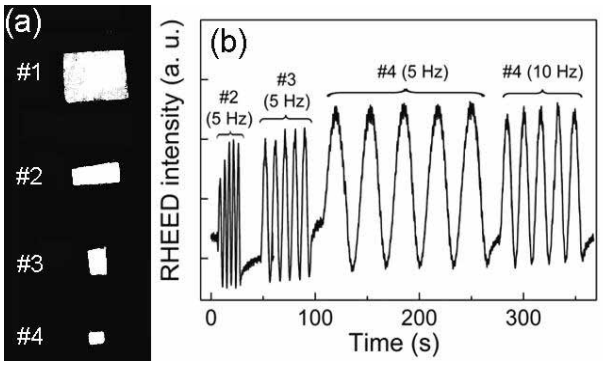

Figure 3. (a) Various laser spots on a target surface used for calibrating the number of laser pulses counted with (b) RHEED-intensity oscillations.

Artificial heterostructures, such as

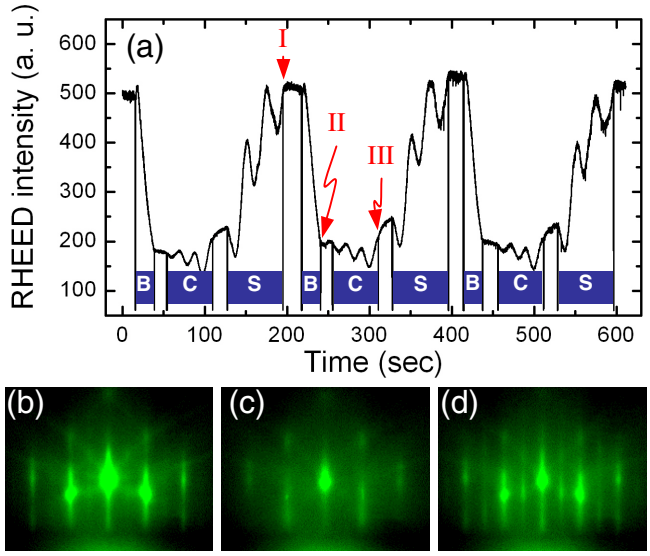

Figure 4. (a) RHEED intensity oscillation of the specular spot from a $(BaTiO_3)_1/(CaTiO_3)_3/(SrTiO_3)_3$ TCS showing a well-controlled surface of each layer. (b), (c), and (d) show RHEED spot images taken at the point I, II, and III, respectively, labeled in (a).

TCSs, are possible on $SrRuO_3$ coated $SrTiO_3$ substrates. Figure 4 shows an example of a well-controlled TCS growth with pronounced RHEED specular spot oscillations and corresponding RHEED spots of a $(BaTiO_3)_1/(CaTiO_3)_3/(SrTiO_3)_3$ tri-color superlattice. It is worth noting that the TCSs have been grown at *10 mTorr* O_2, which is one of highest oxygen pressures used for growing epitaxial titanates with precise control of the layer thickness by RHEED. Growing $BaTiO_3$ deteriorated the surface roughness and interface sharpness as confirmed by RHEED and transmission electron microscopy (not shown) due to the layer-then-island growth mode. Therefore, a "recovery process" is required in order to keep the overall superlattices flat and perfect on the atomic scale. This was achieved by depositing $CaTiO_3$ followed by $SrTiO_3$ with a well-controlled number of laser pulses for growing single or multiple unit cells, because $CaTiO_3$ and $SrTiO_3$ can be easily grown in the layer-by-layer fashion even on a relatively rough surface. The recovery process can be observed in Fig. 4(a). In addition, $CaTiO_3$ revealed a reconstruction feature as shown in Fig. 4(d), despite the otherwise similar behavior of $CaTiO_3$ and $SrTiO_3$. We attribute some of this difference to the use of a ceramic target for $CaTiO_3$

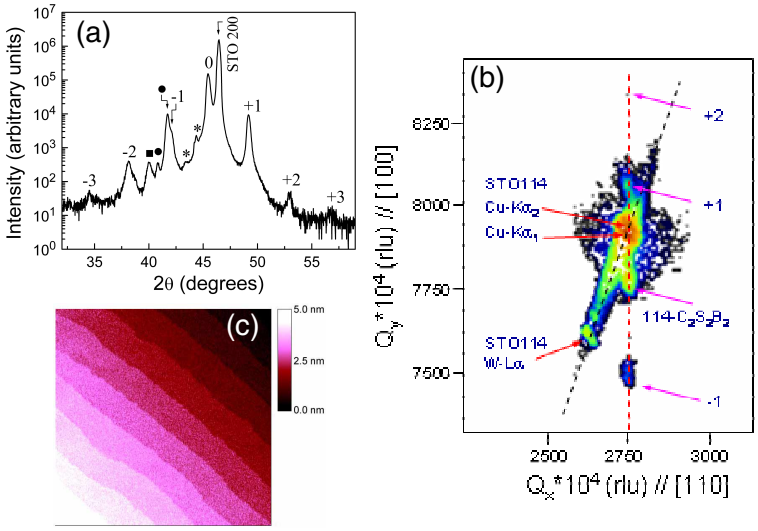

Figure 5. (a) XRD θ-2θ scan and (b) reciprocal space map of a $[(BaTiO_3)_2/(CaTiO_3)_2/(SrTiO_3)_2]_{76}$ superlattice. The latter is recorded with the 114 reflection of $SrTiO_3$. The peaks due to remaining Cu-K_β and W-L_α radiations from the substrate and the layer are labeled as (●) and (*), respectively. The peak labeled as (■) originated from Pt top electrodes. (c) AFM topography (5×5 μm^2) of the surface of the $[(BaTiO_3)_2/(CaTiO_3)_2/(SrTiO_3)_2]_{76}$ superlattice.

and a single-crystal for $SrTiO_3$, leading to the higher surface quality (and thus much brighter RHEED spot) for this layer.

X-ray diffraction θ–2θ scan and reciprocal space map confirmed the high structural quality of superlattices. Figure 5(a) shows a θ–2θ scan of a ~180 nm-thick TCS with a $[(BaTiO_3)_2/(CaTiO_3)_2/(SrTiO_3)_2]_{76}$ structure and Fig. 5(b) is a reciprocal space map [5] of the same sample recorded using the 114 reflection of $SrTiO_3$. Well-spaced superlattice-fringe peaks appear in both the θ–2θ scan and the reciprocal space map. The latter also confirmed that the layers are fully strained (without relaxation). A typical AFM topography image – showing uniform terrace steps with a single unit cell height as shown in Fig. 5(c) – confirms the capability to grow nearly atomically-flat superlattices with complete reproducibility for hundreds of unit cells. TCSs could be grown with thicknesses in excess of one micron with pronounced RHEED oscillations and single-steps on the surface (not shown) *if* the thickness of $BaTiO_3$ was limited to less than three or four unit cells.

CONCLUSIONS

A-site isovalent artificial superlattices using $CaTiO_3$, $SrTiO_3$, and $BaTiO_3$ have been synthesized under precisely controlled growth conditions on single-stepped $SrTiO_3$ substrates covered with $SrRuO_3$ bottom electrodes. RHEED, AFM, and XRD investigations confirm the possibility of growing nearly atomically-flat superlattices with complete reproducibility for thousands of unit cells. Consequently, this work offers a proof-of-principle demonstration that attractive artificial structures and materials can be designed and developed for materials exploration with a view to revealing new physical properties.

ACKNOWLEDGEMENTS

Research sponsored by the U.S. Department of Energy under contract DE-AC05-00OR22725 with the Oak Ridge National Laboratory, managed by UT-Battelle, LLC, as part of a BES NSET initiative on Nanoscale Cooperative Phenomena. Work in part supported by DFG via Group of Researches FOR 404 at Martin-Luther-Universität Halle-Wittenberg.

REFERENCES

1. N. Sai, B. Meyer, and D. Vanderbilt, Phys. Rev. Lett. **84**, 5636 (2000)
2. M. P. Warusawithana, E. V. Colla, J. N. Eckstein, and M. B. Weissman, Phys. Rev. Lett. **90**, 36802 (2003).
3. A. Visinoiu, M. Alexe, H. N. Lee, D. N. Zakharov, A. Pignolet, D. Hesse, and U. Gösele, J. Appl. Phys. **91**, 10157 (2002).
4. J. Choi, C. B. Eom, G. Rijnders, H. Rogalla, and D. H. A. Blank, Appl. Phys. Lett. **79**, 1447 (2001).
5. An ω-offset of about -19.5° was used for recording the reciprocal space map.